Journal of Physics: Conference Series **438** (2013) 012015 doi:10.1088/1742-6596/438/1/012015

Ionization of biomolecular targets by ion impact: input data for radiobiological applications

Pablo de Vera[1,2], Isabel Abril[1], Rafael Garcia-Molina[3] and Andrey V. Solov'yov[2,4]

[1] Departament de Física Aplicada, Universitat d'Alacant, E-03080 Alacant, Spain
[2] Frankfurt Institute for Advanced Studies, Ruth-Moufang-Str. 1, 60438 Frankfurt am Main, Germany
[3] Departamento de Física – Centro de Investigación en Óptica y Nanofísica, Universidad de Murcia, E-30100 Murcia, Spain
[4] On leave from: A.F. Ioffe Physical-Technical Institute, Politechnicheskaya 26, 194021 St. Petersburg, Russia

E-mail: pablo.vera@ua.es

Abstract.

In this work we review and further develop a semiempirical model recently proposed for the ion impact ionization of complex biological media. The model is based on the dielectric formalism, and makes use of a semiempirical parametrization of the optical energy-loss function of bioorganic compounds, allowing the calculation of single and total ionization cross sections and related quantities for condensed biological targets, such as liquid water, DNA and its components, proteins, lipids, carbohydrates or cell constituents. The model shows a very good agreement with experimental data for water, adenine and uracil, and allows the comparison of the ionization efficiency of different biological targets, and also the average kinetic energy of the ejected secondary electrons.

1. Introduction

Ion beam cancer therapy is a powerful emerging tool for treating cancer, specially deep-seated tumours. It makes use of the characteristic energy deposition pattern of ion beams, mainly governed by the electronic stopping force, which is maximum at energies around 100 keV/u, i.e., at the end of the ion's trajectory, giving place to the Bragg peak, a sharp and narrow maximum of the dose near the ion's range. This particular depth-dose profile maximizes the damage produced in tumoral regions, while sparing the energy deposition in surrounding healthy tissues [1].

Although the basic working principles of ion beam cancer therapy are well known, many questions still remain regarding the detailed understanding of the biological outcomes that the physical and chemical stages of the ion propagation in biological media produce. Hadron therapy is, in fact, a complex multiscale problem [2], which involves many different processes in several energy, space and time scales, ranging from nuclear fragmentation reactions until the physical and chemical damage and repair mechanisms of macromolecules such as DNA or proteins, being an important stage the direct electronic excitations and ionizations of these biological molecules by ion impact.

Nowadays, the energy deposition by swift ions in materials of interest in radiotherapy is well known. Particularly, calculations performed within the dielectric formalism [3] have shown to be able of providing accurate values of the electronic stopping force (including many-body and phase effects) in both inorganic (liquid water, metals, semiconductors) [4, 5, 6, 7] and organic (DNA, polymers) materials [8, 9]. These electronic stopping data are needed for detailed simulations of the ion beam propagation through these targets [7, 10]. Nonetheless, one limiting factor of the dielectric formalism is that it includes both electronic excitations and ionizations together, being difficult to extract detailed information on the secondary electron emission. In fact, this information is very relevant, since the major part of the biological damage at a microscopic level is produced by secondary electrons, even the very low energetic ones [11, 12]. Although the dielectric approach has been adapted for describing the electron emission from liquid water induced by ion beams [13, 14], its extension to other relevant biological targets only was achieved very recently [15]. Until then, only methods applicable to atomic targets or small molecules, or limited to some specific targets, projectiles, or energy ranges were available.

In this work we review the main features of the semiempirical method proposed to apply the dielectric formalism to calculate the ionization of complex biological media [15] (section 2), and then we apply it to obtain proton impact ionization data, such as single differential and total cross sections and average kinetic energies of ejected electrons (section 3) of a selection of relevant biological targets. The final conclusions and remarks are given in section 4.

2. Theoretical approach

Several theoretical and semiempirical methods are available to study the electron ejection from atoms and molecules generated by ion impact [16]. Among them, the Binary Encounter Apprximation (BEA) [17] or the Rudd formula [18] are widely used. Nonetheless, these models are restricted to some particular targets or energy ranges: for example, the BEA is quite accurate for atoms or small molecules, whereas its application is difficult for large macromolecules. Moreover, it is not valid for very low ion energies (where two-center effects in the collision are not taken into account) and for high energies (where dipole interactions play a major role and are not considered). On the other hand, the Rudd formula is valid for a wide energy range, but its application is limited to some selected targets for which its parameters have been fitted to experimental data [16]. Regarding other more sophisticated theoretical models, such as quantum models like the Continuum-Distorted-Wave–Eikonal-Initial-State (CDW-EIS) method [19, 20], or the Classical Trajectory Monte Carlo (CTMC) method [21], their application to large biological molecules is computationally quite complex and expensive.

The dielectric formalism (based on the Plane Wave Born Approximation, PWBA) [3] provides a first perturbative theoretical framework in which the electronic magnitudes can be analytically treated for a wide energy range, for various charged projectiles such as protons, heavier ions or electrons, and where many-body and condensed phase effects are taken into account.

2.1. Ionization of the outer shell electrons: dielectric formalism

According to the dielectric formalism, the macroscopic single differential cross section (SDCS), or inverse mean free path, for the ejection of an electron with kinetic energy W from the electronic i-shell of the target, by a projectile of kinetic energy T, mass M_1 and charge Z_1 is [22]

$$\left.\frac{\mathrm{d}\Lambda(T,W)}{\mathrm{d}W}\right|_i = \frac{e^2}{\pi\hbar^2}\frac{M_1 Z_1^2}{T}\int_{k_-}^{k_+}\frac{\mathrm{d}k}{k}\mathrm{Im}\left[\frac{-1}{\epsilon(k,B_i+W)}\right]_i , \tag{1}$$

where E and $\hbar k$ are, respectively, the energy and momentum transfers. We have used $E = B_i + W$, being B_i the binding energy of the i-shell. The excitation spectrum of the target enters in this equation through the quantity known as the energy-loss function (ELF),

Table 1. Physical properties of the biological targets studied in this work. Atomic compositions have been converted from mass percentage compositions from Ref.[27] (except otherwise stated), Z_2 and A_2 are the sum of the atomic and mass numbers of all the atoms in each formula, while $\mathcal{Z}_2$ is Z_2 divided by the number of atoms in the formula. Densities and $\overline{B}$ values were set equal to 1.00 g/cm^3 and 20 eV, respectively, when they were unknown.

Material (formula)	Z_2	A_2	$\mathcal{Z}_2$	ρ (g/cm^3)	$\overline{B}$ (eV)
Liquid water (H_2O)	10	18.02	3.33	1.00	18.13 [13]
Adenine ($C_5H_5N_5$)	70	135.13	4.67	1.35 [24]	20.44 [37]
Guanine ($C_5H_5O_1N_5$)	78	151.13	4.87	1.58 [24]	21.09 [37]
Thymine ($C_5H_6O_2N_2$)	66	126.11	4.40	1.36 [31]	20.29 [37]
Cytosine ($C_4H_5O_1N_3$)	58	111.10	4.46	1.30 [24]	20.47 [37]
Uracil ($C_4H_4O_2N_2$)	58	112.09	4.83	1.40 [31]	20.73 [37]
DNA backbone ($C_5H_{10}O_5P_1$)	95	181.10	4.52	1.00	19.14 [37]
DNA ($C_{20}H_{27}O_{13}N_7P_2$) [28]	330	635.41	4.78	1.35 [28]	20.00
Protein ($C_{142.56}H_{209.97}O_{44.09}N_{38.92}S_1$)	1706.49	3206.50	3.91	1.35	20.00
Lipid ($C_{9.44}H_{17.18}O_1$)	81.87	146.78	2.96	0.92	20.00
Carbohydrate ($C_{1.20}H_{2.00}O_1$)	17.21	32.45	4.10	1.56	20.00
Cell nucleus ($C_{60.07}H_{843.06}O_{371.77}N_{18.31}P_{6.73}S_1$)	4422.75	8016.25	3.40	1.00	20.00
Cytoplasm ($C_{1926.40}H_{8105.31}O_{2724.83}N_{138.76}P_1S_{5.80}Na_{3.71}Cl_{3.49}K_{4.16}$) [29]	42720.60	77434.50	3.31	1.00	20.00

$\mathrm{Im}\left[-1/\epsilon(k, B_i + W)\right]$, where $\epsilon(k, B_i + W)$ is the complex dielectric function of the target. The sub-index i in eq.(1) refers to the contribution of the i electronic shell to the ELF. The integration limits, imposed by conservation laws, are $k_\pm = \sqrt{2M_1}(\sqrt{T} \pm \sqrt{T - E})$. The macroscopic cross section, Λ, is related to the microscopic one, σ, through $\Lambda = \mathcal{N}\sigma$, being $\mathcal{N}$ the molecular density of the target.

Once the SDCS is known, other key radiobiological quantities can be calculated from it, such as the total ionization cross section (TICS)

$$\Lambda(T) = \int_0^\infty \frac{\mathrm{d}\Lambda(T, W)}{\mathrm{d}W}\mathrm{d}W \ , \tag{2}$$

and the average energy of the emitted electrons

$$W_{\mathrm{average}}(T) = \frac{1}{\Lambda(T)} \int_0^\infty W \frac{\mathrm{d}\Lambda(W)}{\mathrm{d}W}\mathrm{d}W \ . \tag{3}$$

The advantage of the dielectric formalism is that, provided that the ELF is experimentally known, many-body interactions and target physical-state effects are naturally included in the subsequent calculations. Therefore, the key magnitude to compute the ionization cross sections is the target ELF over the whole energy and momentum transfer plane (the so-called Bethe surface). In the following section we discuss how to obtain the ELF of biological materials in a simple and efficient manner. Once the ELF is known, we need a criterion to split it in excitations and ionizations, which will be explained in section 2.3.

2.2. The energy-loss function of bioorganic targets

The ELF for all the electronic excitations and ionizations of a target can be experimentally determined from optical data (zero momentum transfer, $k = 0$) or X-ray and electron energy-

loss experiments ($k \neq 0$). Optical data are available for a large number of materials, among which only a few are organic or biological compounds.

Regarding the latter ones, Tan and co-workers [23, 24] noticed that the optical-ELF of 13 bioorganic condensed compounds and liquid water at low energies (corresponding to the excitation of the outer shell electrons) are rather similar, with an intense peak around 20–25 eV, and sometimes with other small peaks at lower energies. This fact led them to the idea that the experimental optical ELF of the outermost electrons of organic compounds can be parametrized with a single-Drude function

$$\mathrm{Im}\left[\frac{-1}{\epsilon(k=0,E)}\right] = \frac{a(Z_2)E}{[E^2 - E_\mathrm{p}^2(\mathcal{Z}_2)]^2 + \gamma^2(\mathcal{Z}_2)E^2} \ , \tag{4}$$

where $a(Z_2)$ (in eV^3), $E_\mathrm{p}(\mathcal{Z}_2)$ (in eV) and $\gamma(\mathcal{Z}_2)$ (in eV) represent the intensity, position and width of the single-Drude ELF. Using the experimental optical ELF of the 14 bioorganic compounds, $E_\mathrm{p}(\mathcal{Z}_2)$ and $\gamma(\mathcal{Z}_2)$ were parametrized as a function of the mean atomic number of the target, $\mathcal{Z}_2$ (i.e., the number of electrons per formula divided by the number of atoms) [23],

$$E_\mathrm{p} = 19.927 + 0.9807 \cdot \mathcal{Z}_2 \, , \tag{5}$$

$$\gamma = 13.741 + 0.3215 \cdot \mathcal{Z}_2 \, . \tag{6}$$

The remaining parameter, $a(Z_2)$, can be simply obtained by imposing the accomplishment of the f-sum rule [25], linked to the number of electrons in the target, Z_2 (i.e., the sum of the atomic numbers of all the atoms in the formula); of course, the inner shells also contribute to the number of electrons. In this parametric approach, eq.(4) is used for transferred energies below 40 eV, and above 50 eV ELF is obtained from X-ray atomic scattering factors [26], ensuring that the inner-shell electrons are considered for the calculation of the parameter $a(Z_2)$. Between 40 and 50 eV, a parabola is used to link Eq.(4) with the X-ray data (see Ref.[23] for a detailed explanation).

This method allows the prediction of the optical ELF for an arbitrary bioorganic compound in the optical limit ($k = 0$), provided that the atomic composition (for calculating $\mathcal{Z}_2$) and density (which affects the f-sum rule) are known. This information is easily accessible for any material. Specifically, the average composition and density of a large number of biological targets is compiled in the ICRU Report 46 [27]. We summarize in Table 1 the physical properties of the representative biological materials studied in this work, which have been obtained from Ref. [27], except for DNA [28] and the cytoplasm [29]. The average mass composition of each target has been converted to number of atoms per formula, assigning 1 atom to the less abundant component, in order to calculate the values of Z_2, A_2 and $\mathcal{Z}_2$. In Fig. 1 we show the predicted optical ELFs for liquid water and solids dry DNA, adenine, guanine, thymine and uracil, together with the available experimental data [28, 30, 31, 32, 33]. As it can be seen, the agreement is very good in practically all cases, except for liquid water, where the asymmetry of the experimental ELF can not be reproduced with a single-Drude function.

Once the ELF is known in the optical limit, we need to extend it to $k \neq 0$ in order to obtain the whole Bethe surface. There are several methods available to obtain the ELF at finite values of the momentum transfer [34]. Among them, we use here a simple dispersion relation introduced by Ritchie and Howie, derived from the similarity between the Drude function (eq.(4)) at $k = 0$ and $\gamma = 0$ with the Lindhard function for the free electron gas [35], which simply consists in replacing E_p in eq.(4) by

$$E_\mathrm{p}(k) = E_\mathrm{p}(k=0) + \alpha\frac{\hbar^2k^2}{2m_\mathrm{e}} \approx E_\mathrm{p}(k=0) + \frac{\hbar^2k^2}{2m_\mathrm{e}} \ , \tag{7}$$

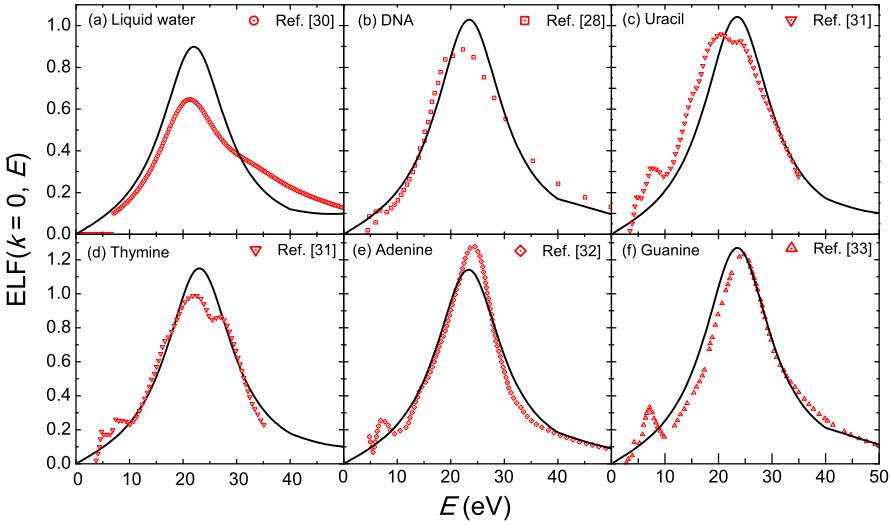

Figure 1. Comparison of the optical-ELF obtained through the parametric model of Eq.(4) (solid lines) with available experimental data (symbols) for: (a) liquid water [30], (b) solid DNA [28], (c) solid uracil [31], (d) solid thymine [31], (e) solid adenine [32], and (f) solid guanine [33].

where $m_\urcorner$ is the electron mass and $\alpha = 6E_{\rm Fermi}/5E_{\rm plasmon}$, being $E_{\rm Fermi}$ and $E_{\rm plasmon}$ the nominal Fermi and plasmon energies of the free electron gas [36]. $\alpha \approx 1$ for liquid water [34], and we have kept this value for the rest of biomaterials for the sake of simplicity. No dispersion relation was assumed for the damping coefficient γ. Although this extension of the ELF to $k \neq 0$ is only an approximation, its accuracy is in the order of other approximations made in this work.

2.3. Ionization of the outer-shell and inner-shell electrons

The SDCS given by eq.(1) is not only valid for the ionization of the i-shell, but it can also account for excitations. It can describe the ionization of an electronic shell i provided that we know the contribution of the ionization of this shell to the total ELF. Since the ELF was obtained in the previous section from an empirical parametrization to experimental ELFs, which include all the possible excitations and ionizations of the target, we need some criterion to distinguish the ionizations from the excitations and evaluate the electron production cross sections.

One case already studied is liquid water: its ELF has been parametrized in contributions of excitations and ionizations of different shells in the works by Dingfelder [13] and Emfietzoglou [14]. Basically, these authors used the experimental excitation spectrum, represented by the imaginary part of the dielectric function, and fitted its different peaks by normal and derivative Drude functions in order to identify and reproduce each resonance, making use of information on the excitation and ionization energies of each shell.

This procedure is satisfactory for water, which only has four outer molecular orbitals. Nonetheless, the generalization of such a parametrization for large and complex macromolecules is not a trivial issue. For these reason, we introduce here a further approximation. If one looks at the existing parametrizations performed for liquid water [13, 14], it can be seen that the excitations are practically confined at low transferred energies, while at high energies only ionizations remain. Therefore, we can estimate a mean binding energy, $\overline{B}$, from the ionization thresholds of all the outer electronic shells, and assume that ionizations will only occur at energies above this threshold (the electron being ejected with an energy $W = E - \overline{B}$), and excitations only below it. This mean binding energy is 18.13 eV for liquid water [13]; in fact, a few electronvolts above this energy excitations practically vanish, while only ionizations remain. Moreover, the

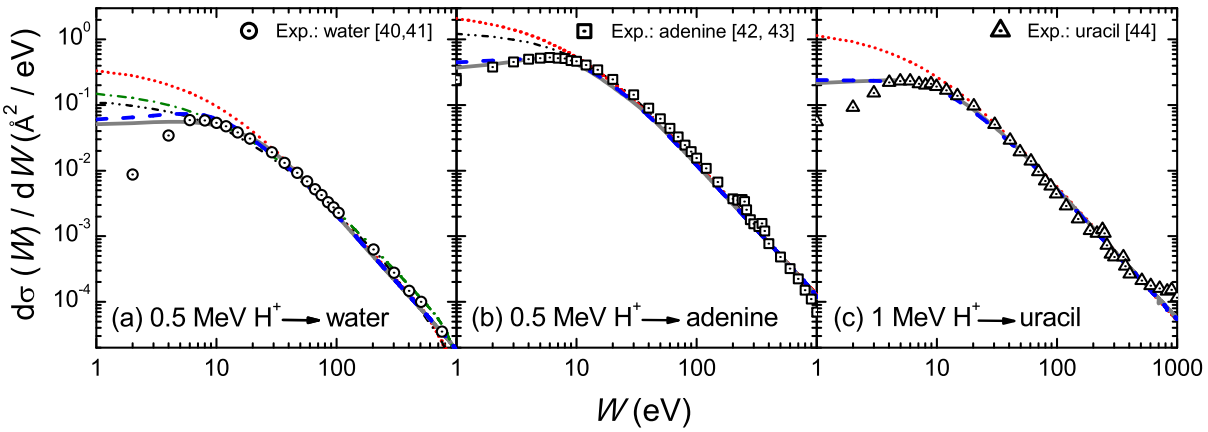

Figure 2. SDCS for ionization of (a) water, (b) adenine and (c) uracil by protons of a given energy. Symbols represent experimental data [40, 41, 42, 43, 44], while solid (dashed) lines are our calculations within the dielectric formalism using the experimental (parametrized) optical ELF of the target, as described in the text. Dotted lines are calculations performed within the BEA model, while the dash-dotted line is the result of the Rudd formula for liquid water. The dash-dot-dotted lines are other calculations for the water molecule (Classical Trajectory Monte Carlo method [21]) and adenine molecule (quantum mechanical calculations [20]).

use of such a mean binding energy is justified, since the difference between the actual binding energies of each shell and the mean value will be of the order of a few electronvolts, which is negligible for the further transport of the secondary electrons. Finally, it will be seen in section 3 that this approximation yields good results in comparison with the available experimental data.

Information on the ionization energies of the different shells of biological molecules can be easily obtained from the literature, from databases or from quantum chemistry calculations. In particular, there is information available for liquid water [13], DNA components [37], amino acids [38] and other organic molecules [39]. From these data we have calculated the mean binding energies of the targets studied in this work, which are collected in Table 1. Since the values of $\overline{B}$ are always close to 20 eV, we have set this value for the complex targets for which we do not have direct information, such as the DNA molecule, proteins or the cell nucleus.

Although the major contribution to the ionization cross section comes from the outer shells, the inner shells can also have noticeable effects in the calculation of some quantities, such as the average energy of ejected electrons, eq.(3). So far we have dealt only with outer shell electrons. For the inner shells, which can be regarded as isolated cores, where chemical and phase effects are less important, simpler theoretical models such as the BEA can be used instead. For describing the SDCS of the inner shells, in this work we have used a simple BEA equation [16], where the binding and mean kinetic energies of each shell, B_i and U_i respectively, have been obtained from a database by the National Institute of Standards and Technology (NIST) [39].

3. Results and discussion

We have calculated ionization cross sections for proton impact in several representative biological targets using the models described above, i.e., the dielectric formalism with the ELF parametrization of bioorganic compounds and the mean ionization energy for the outer shell electrons, and the BEA for the inner shell electrons. The compositions, densities and mean binding energies of the targets are summarized in Table 1.

Figure 2 shows the SDCS calculated with the proposed model for protons of a given energy in liquid water, solid adenine and solid uracil, compared with available experimental data for

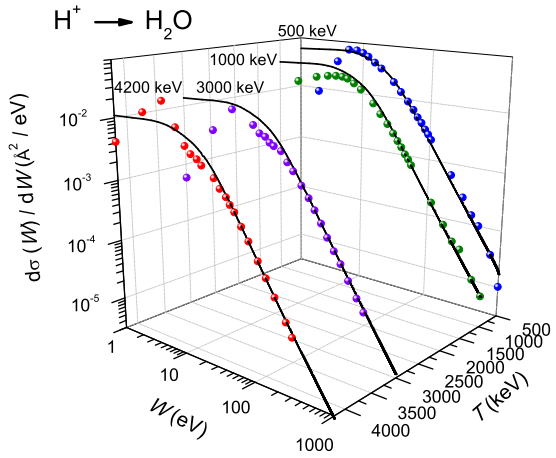

Figure 3. Single differential cross sections (SDCS) for ionization of liquid water by protons of several energies obtained with the present model. Symbols represent experimental data for water vapour [40, 41].

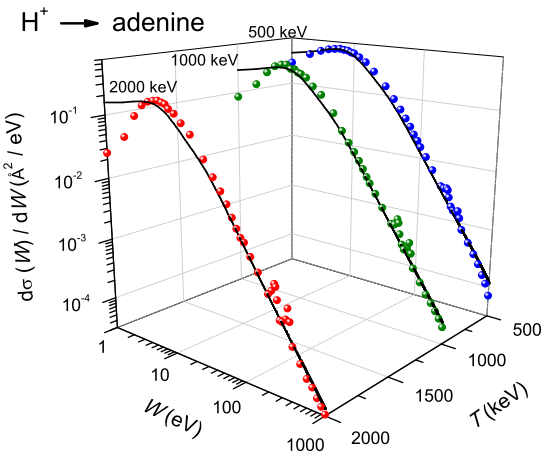

Figure 4. Single differential cross sections (SDCS) for ionization of solid adenine by protons of several energies obtained with the present model. Symbols represent experimental data for adenine vapour [42, 43].

the corresponding gas phases [40, 41, 42, 43, 44]. Although the calculations are performed for condensed phases, we do not know experimental data for condensed targets with which we can compare. Nonetheless, the agreement with the gas data is excellent at almost all ejection energies, except for some differences at very low electron energies. These differences could be due to phase effects or to the extreme difficulty of experimentally determining these energies.

In Fig. 2 we plot by solid lines the calculations performed using the experimental optical ELF of these materials, while dashed lines depict the calculations done using the predicted ELF by the parametric model of Ref. [23]. The comparison of both calculations allows us to estimate the error coming from the ELF prediction. As it can be seen, the differences are very small for adenine and uracil. Larger differences are observed in the case of liquid water at very low energies, where the parametric model is not able of reproducing the asymmetry of the experimental ELF. In this case, the error in the maximum of the SDCS is around 30 %, which is not so big taking into account the predictive power of the method. In any case, it is preferable to use the experimental ELF when it is available, like in the cases shown in Fig. 1, being the method in this case more reliable. We show in Figs. 3 and 4 our calculated SDCS for proton beams at several energies in liquid water and solid adenine, respectively, using their experimental ELF, finding an overall agreement with experiments.

The comparison of our calculations with other models also gives support to our methodology. In Fig. 2 we also show by dotted lines the SDCS calculated for the gas phases within the BEA model, while the dash-dotted line of Fig. 2(a) is the SDCS obtained with the Rudd formula for water vapour and the dash-dot-dotted lines of Fig. 2(a) and (b) are *ab initio* calculations, within the Classical Trajectory Monte Carlo method for water [21], and quantum mechanical calculations for adenine [20]. The agreement between all the models and experiments is rather good at high energies, but at low energies, say below 10–20 eV, our calculations seem to agree better with the experimental data. The causes of these discrepancies (especially with the *ab initio* calculations) deserve more attention, but a possible explanation of our better agreement is that we are considering a more realistic target excitation spectrum through its ELF.

In Fig. 5 we show our calculated TICS (eq. (2)) for all the materials of Table 1: Fig. 5(a) shows the macroscopic cross sections (i.e., inverse mean free paths) for liquid water, DNA, protein, lipid, carbohydrate, cytoplasm and the cell nucleus, while Fig. 5(b) shows the microscopic cross sections (i.e., TICS per molecule) of the DNA/RNA molecular components adenine, thymine, cytosine, guanine, uracil

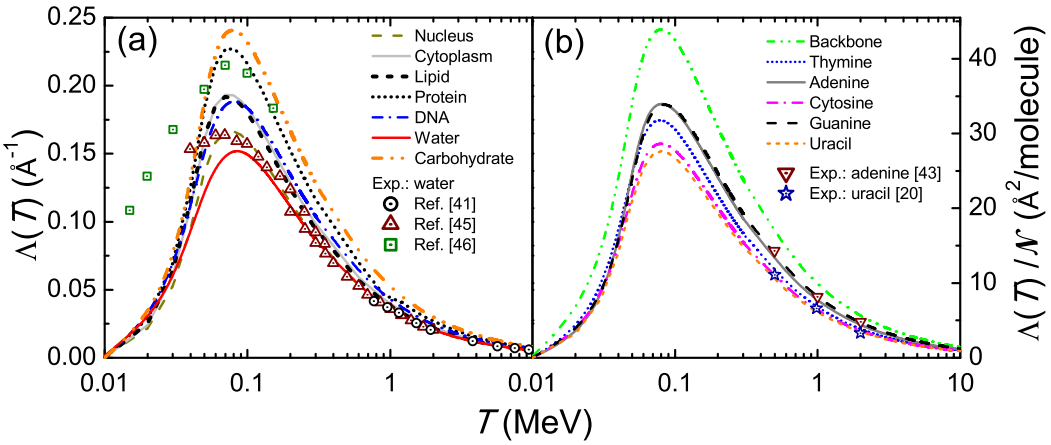

Figure 5. (a) Macroscopic TICS (inverse mean free path), and (b) microscopic TICS per molecule for protons in several biological materials in the condensed phase, compared with experimental data in water vapour [41, 45, 46], adenine vapour [43] and uracil vapour [20].

and sugar-phosphate backbone. Also shown in these figures are experimental data for the water, adenine and uracil molecules in the gas phase [20, 41, 43, 45, 46]. As it can be seen, our calculations nicely agree with the experiments, except for some differences around 100 keV in the case of water measurements from Refs. [45] and [46]; the slight disagreement with the measurements by Rudd *et al.* [45] could be due to phase effects, and also to the fact that the dielectric formalism (which is based on the first Born approximation) starts to lose validity at these low energies. In any case, the dispersion between the measurements by Rudd *et al.* [45] and by Bolorizadeh *et al.* [46] is remarkable.

The information depicted in Fig. 5 is quite interesting, since it shows the different sensitivities of each target to ion impact ionization. Among the macroscopic targets shown in Fig. 5(a), it seems that carbohydrates and protein has the largest TICS, probably influenced by their bigger densities (see Table 1). Regarding the cell nucleus, it has a TICS which is practically identical to that of liquid water in almost all the energy range, but with slight differences in the maximum. Nonetheless, these differences are too small (within the uncertainties of the ELF prediction for liquid water) that it is not possible to conclude that the cell nucleus is more sensible than liquid water itself. Nonetheless, the cytoplasm, lipid and DNA show TICS larger than liquid water and the cell nucleus, a fact that could indicate a larger ionization probability of these targets. It is remarkable the possible effect of the larger density of the DNA, but here lipids and the cytoplasm are considered to have densities similar to that of liquid water. Among the microscopic TICS shown in Fig. 5(b), now the density is not a factor (TICS per molecule are shown), and we still observe differences in their cross sections, being remarkable that the DNA sugar-phosphate backbone shows the largest ionization probability. Perhaps, in this case, the dominant factor is the number of electrons per molecule.

Other interesting quantity which can be calculated for several biological media is the average energy of secondary electrons. According to eq.(3), the high energy transfers will be more relevant in this calculations, so ionization of the inner shells (introduced here through the BEA) will play a noticeable role. In Fig. 6 we show our results for seven representative biological targets: liquid water, dry DNA, protein, lipid, cell nucleus, cytoplasm, and carbohydrate. We also include other calculation for liquid water from Ref. [47], which agrees quite well with our water curve. Our results indicate that the differences in W_{average} between these targets is not very significant, spanning from the maximum of liquid water and the minimum of proteins, which are around 55 and 45 eV, respectively, at 1 MeV proton impact.

4. Summary and conclusions

In this work we review, explain in more detail and expand our semiempirical method proposed to evaluate the ion impact ionization cross sections for condensed complex biological targets based on the dielectric

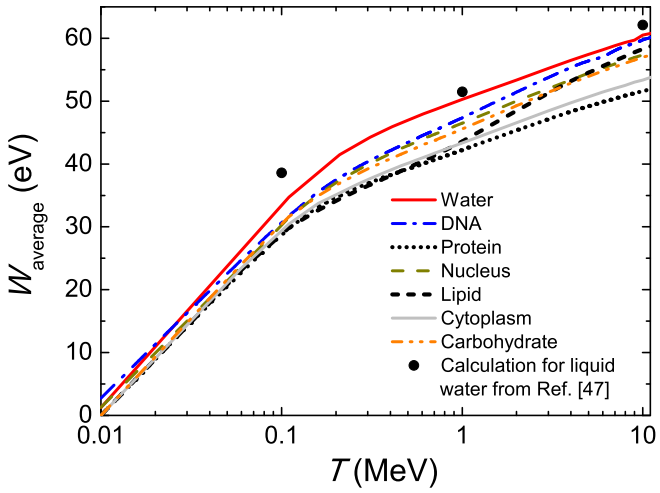

Figure 6. Average kinetic energy of the secondary electrons ejected from different biological materials by proton impact, calculated with our semiempirical model for the outer shell electrons, and with the BEA for the inner shells.

formalism and a semiempirical parametrization of the experimental optical ELF of organic compounds [15]. Calculations are extended to a broad selection of representative biological targets (liquid water, DNA, proteins, lipids, carbohydrates, the cell nucleus and cytoplasm, and the DNA/RNA molecular components adenine, guanine, cytosine, thymine, uracil and sugar-phosphate backbone), including the contribution from the inner shells to properly perform the calculation of the average energy of secondary electrons, besides the single differential and total cross sections. Our calculations show an excellent agreement with experimental data in the gas phase for water, adenine and uracil, and they also agree with other semiempirical, theoretical and *ab initio* calculations at high ejection energies. At low energies, our model seems to agree better than the others with the experimental data. We evaluate ionization cross sections and average energies of secondary electrons for all the cited targets, showing some differences between their ionization efficiency, but a quite similar behaviour of the average energy of secondary electrons. This method will be extended in future works to account for heavier ions in different charge states, and also for electron impact.

Acknowledgments

The authors want to thank fruitful discussions and helpful data provided by Drs. E. Surdutovich, E. Scifoni, D. Emfietzoglou and C. Champion. We recognize the financial support from the Spanish Ministerio de Economía y Competitividad and the European Regional Development Fund within the Project FIS2010–17225 and from the Conselleria d'Educació, Cultura i Esport de la Generalitat Valenciana for granting PdV within the VALi+d program. Support from the COST Action MP1002 NanoIBCT is greatfully acknowledged.

[1] Kraft G 2000 *Progr. Part. Nucl. Phys.* **45** S473.
[2] Solov'yov A V, Surdutovich E, Scifoni E, Mishustin I and Greiner W 2009 *Phys. Rev. E* **79** 011909.
[3] Lindhard J 1954 *K. Dan. Vidensk. Selsk. Mat. Fys. Medd.* **28** (8).
[4] Heredia-Avalos S, Garcia-Molina R, Fernández-Varea J M and Abril I 2005 *Phys. Rev. A* **72** 052902-1.
[5] Heredia-Avalos S, Moreno-Marín J C, Abril I and Garcia-Molina R 2005 *Nucl. Instr. Meth. B* **230** 118.
[6] Garcia-Molina R, Abril I, Denton C D, Heredia-Avalos S, Kyriakou I and Emfietzoglou D 2009 *Nucl. Instr. Meth. B* **267** 2647.
[7] Garcia-Molina R, Abril I, Heredia-Avalos S, Kyriakou I and Emfietzoglou D 2011 *Phys. Med. Biol.* **56** 6475.
[8] Abril I, Garcia-Molina R, Denton C D, Kyriakou I and Emfietzoglou D 2011 *Rad. Res.* **255** 247.
[9] de Vera P, Abril I and Garcia-Molina R 2011 *J. Appl. Phys.* **109** 094901.

[10] de Vera P, Abril I and Garcia-Molina R 2013 *Appl. Rad. Isot.*, in press. DOI: 10.1016/j.apradiso.2013.01.023
[11] Boudaïffa B, Cloutier P, Hunting D, Huels M A and Sanche L 2000 *Science* **287** 1658.
[12] Pan X, Cloutier P, Hunting D and Sanche L 2003 *Phys. Rev. Lett.* **90** 208102.
[13] Dingfelder M, Hantke D, Inokuti M and Paretzke H G 1998 *Rad. Phys. Chem.* **53** 1.
[14] Emfietzoglou D 2003 *Rad. Phys. Chem.* **66** 373.
[15] de Vera P, Garcia-Molina R, Abril I and Solov'yov A V 2013 *Phys. Rev. Lett.*, in press (2013).
[16] International Commission on Radiation Units and Measurements 1996 *Secondary Electron Spectra from Charged Particle Interactions* (ICRU Report 55) (Bethesda, MD: ICRU).
[17] Vriens L 1967 *Proc. Phys. Soc. London* **90** 935.
[18] Rudd M E, Kim Y-K, Madison D H and Gay T J 1992 *Rev. Mod. Phys.* **64** 441.
[19] Crothers D S F and McCann J F 1983 *J. Phys. B: At. Mol. Phys.* **16** 3229.
[20] Galassi M E, Champion C, Weck P F, Rivarola R D, Fojón O and Hanssen J 2012 *Phys. Med. Biol.* **57** 2081.
[21] Errea L F, Illescas C, Méndez L and Rabadán I 2013 *Phys. Rev. A* **87** 032709.
[22] Emfietzoglou D 2012 Inelastic scattering of charged particles in condensed media: a dielectric theory perspective, Section III in *Interaction of Radiation with Matter*, edited by H. Nikjoo, S. Uehara, and D. Emfietzoglou (Boca Raton: CRC Press).
[23] Tan Z, Xia Y, Zhao M, Liu X, Li F, Huang B and Ji Y 2004 *Nucl. Instr. Meth. B* **222** 27.
[24] Tan Z, Xia Y, Zhao M and Liu X 2006 *Nucl. Instr. Meth. B* **248** 1.
[25] Altarelli M and Smith D Y 1974 *Phys. Rev. B* **9** 1290.
[26] Henke B L, Gullikson E M and Davis J C 1993 *At. Data Nucl. Data Tables* **54** 181. The ASCII files for the scattering factors of the different elements can be downloaded from `http://henke.lbl.gov/optical_constants/asf.html`
[27] International Commission on Radiation Units and Measurements 1992 *Photon, Electron, Proton and Neutron Interaction Data for Body Tissues* (ICRU Report 46) (Bethesda, MD: ICRU).
[28] Inagaki T, Hamm R N, Arakawa E T and Painter L R 1974 *J. Chem. Phys.* **61** 4246.
[29] Byrne H L, McNamara A L, Domanova W, Guatelli S and Kuncic Z 2013 *Phys. Med. Biol.* **58** 1251.
[30] Hayashi H, Watanabe N, Udagawa Y and Kao C C 2000 *Proc. Nat. Acad. Sci. USA* **97** 6264.
[31] Isaacson M 1972 *J. Chem. Phys.* **56** 1803.
[32] Emerson L C, Williams M W, Tang I'lan, Hamm R N and Arakawa E T 1975 *Radiat. Res.* **63** 235.
[33] Arakawa E T, Emerson L C, Juan S I, Ashley J C and Williams M W 1986 *Photochem. Photobiol.* **44** 349.
[34] Garcia-Molina R, Abril I, Kyriakou I and Emfietzoglou D 2012 Energy Loss of Swift Protons in Liquid Water: Role of Optical Data Input and Extension Algorithms, Chapter 15 in *Radiation Damage in Biomolecular Systems*, edited by G. García Gómez-Tejedor and M. C. Fuss (Dordrecht: Springer).
[35] Ritchie R H and Howie A 1977 *Philos. Mag.* **36** 463.
[36] Ashcroft N W and Mermin N D 1976 *Solid State Physics* (Fort Worth: Saunders College Publishing).
[37] Bernhardt Ph and Paretzke H G 2003 *Int. J. Mass Spectr.* **223-224**.
[38] Peudon A, Edel S and Terrisol M 2006 *Radiat. Prot. Dos.* **122** 128.
[39] Kim Y-K, Irikura K K, Rudd M E, Ali M A, Stone P M, Chang J, Coursey J S, Dragoset R A, Kishore A R, Olsen K J, Sansonetti A M, Wiersma G G, Zucker D S and Zucker M A 2004 *Electron-Impact Ionization Cross Section for Ionization and Excitation Database* (version 3.0) (Gaithersburg, MD: National Institute of Standards and Technology). Available online: `http://www.nist.gov/pml/data/ionization/index.cfm`
[40] Toburen L H and Wilson W E 1977 *J. Chem. Phys.* **66** 5202.
[41] Wilson W E, Miller J H, Toburen L H and Manson S T 1984 *J. Chem. Phys.* **80** 5631.
[42] Iriki Y, Kikuchi Y, Imai M and Itoh A 2011 *Phys. Rev. A* **84** 032704.
[43] Iriki Y, Kikuchi Y, Imai M and Itoh A 2011 *Phys. Rev. A* **84** 052719.
[44] Iriki Y, Kikuchi Y, Doi K, Imai M and Itoh A 2012 *J. Phys.: Conf. Series* **388** 102041.
[45] Rudd M E, Goffe T V, DuBois R D and Toburen L H 1985 *Phys. Rev. A* **31** 492.
[46] Bolorizadeh M A and Rudd M E 1986 *Phys. Rev. A* **33** 888.
[47] Pimblott S M, LaVerne J A 2007 *Radiat. Phys. Chem.* **76** 1244.